Journal of Biomedical Optics

BiomedicalOptics.SPIEDigitalLibrary.org

In vivo super-resolution imaging of transient retinal phototropism evoked by oblique light stimulation

Yiming Lu
Changgeng Liu
Xincheng Yao

SPIE.

Yiming Lu, Changgeng Liu, Xincheng Yao, "*In vivo* super-resolution imaging of transient retinal phototropism evoked by oblique light stimulation," *J. Biomed. Opt.* **23**(5), 050502 (2018), doi: 10.1117/1.JBO.23.5.050502.

In vivo super-resolution imaging of transient retinal phototropism evoked by oblique light stimulation

Yiming Lu,[a] Changgeng Liu,[a] and Xincheng Yao[a,b,*]
[a]University of Illinois at Chicago, Department of Bioengineering, Chicago, Illinois, United States
[b]University of Illinois at Chicago, Department of Ophthalmology and Visual Sciences, Chicago, Illinois, United States

Abstract. Rod-dominated transient retinal phototropism (TRP) has been observed in freshly isolated retinas, promising a noninvasive biomarker for objective assessment of retinal physiology. However, *in vivo* mapping of TRP is challenging due to its subcellular signal magnitude and fast time course. We report here a virtually structured detection-based super-resolution ophthalmoscope to achieve subcellular spatial resolution and millisecond temporal resolution for *in vivo* imaging of TRP. Spatiotemporal properties of *in vivo* TRP were characterized corresponding to variable light intensity stimuli, confirming that TRP is tightly correlated with early stages of phototransduction. [DOI: 10.1117/1.JBO.23.5.050502]

Keywords: functional imaging; super-resolution microscopy; ophthalmoscopy; retina; photoreceptor.

Paper 180148LR received Mar. 15, 2018; accepted for publication Apr. 19, 2018; published online May 11, 2018.

It has been well established that many eye diseases, such as age-related macular degeneration (AMD) and retinitis pigmentosa (RP), can impair retinal photoreceptors and inner neurons to cause vision loss.[1,2] As physiological abnormalities may occur before detectable morphological distortions, functional imaging of retinal physiology is essential for early diagnosis of eye diseases and reliable assessment of treatment outcomes. Although psychophysical and electrophysiological methods can be used for functional examination of the visual system, they suffer from low signal specificity or insufficient spatial resolution.[3–6] Therefore, a high-resolution method for objective examination of photoreceptor physiology is desirable to advance early diagnosis of AMD, RP, etc. Particularly, rod photoreceptors are known to be more vulnerable, compared with cone photoreceptors, in early AMD and RP.[1,2]

Rod-dominated transient retinal phototropism (TRP) has been recently observed in freshly isolated amphibian and mammal retinas stimulated by oblique visible light illumination.[7] Functional OCT of living eye-cups and time-lapse microscopy of retinal slices revealed that TRP has an anatomic origin within the outer segment (OS),[8] presumably caused by localized shrinkage of rod OSs.[9] Comparative electrophysiological investigation into isolated retina further identified the physiological source of TRP to the phototransduction processes before hyperpolarization of the rod photoreceptor.[10] Therefore, TRP provides a noninvasive biomarker for objective assessment of rod function, promising a high-resolution method for early detection of AMD, RP, etc. However, *in vivo* mapping of the rod-dominated TRP is challenging due to its rapid time course and subcellular movement magnitude.[7,9,10]

We recently demonstrated a super-resolution scanning laser ophthalmoscope for *in vivo* imaging of frog retina.[11] The custom-designed ophthalmoscope employed virtually structured detection (VSD) to achieve subcellular level spatial resolution, and it combined a rapid line-scan strategy to realize millisecond-level temporal resolution. In this paper, we report the first *in vivo* observation of TRP using the VSD-based line-scan super-resolution ophthalmoscope. Temporal dynamics of *in vivo* TRP correlated with variable stimulus intensities was characterized to verify the physiological origin of TRP.[12]

Adult northern leopard frogs (*Rana Pipiens*) were used for this study. The frogs were first dark-adapted for at least 4 h prior to *in vivo* imaging and then anesthetized through the skin. After confirmation of anesthesia, the frog was fixed in a custom-built holder and the pupils were fully dilated with topical atropine (1%) and phenylephrine (2.5%) for *in vivo* imaging. All experiments in this research were performed following the protocols approved by the Animal Care Committee at the University of Illinois at Chicago, and conformed to the statement on the use of animals in ophthalmic and vision research, established by the Association for Research in Vision and Ophthalmology.

Figure 1(a) shows a schematic diagram of the line-scan super-resolution ophthalmoscope. The light source is a near-infrared superluminescent diode (SLD-35-HP; Superlum Ireland, Inc.) with a center wavelength at 830 nm and a bandwidth of 60 nm. The light entering the frog pupil had a ∼2-mm beam diameter, with a ∼2.5-mW power. A focused line in the *X*-direction, produced by a cylindrical lens, scanned across the retina in the *Y*-direction under the control of a scanning galvanometer mirror (GVS001; Thorlabs, Inc.). Due to the line focus illumination and microsecond-level exposure time, the illumination power applied to the retina was well below the maximum permissible exposure determined by the ANSI and IEC laser safety standards.[13–15] The line profile reflected from the retina was recorded by a high-speed two-dimensional (2-D) CMOS camera (FastCam Mini AX50; Photron, Inc.). To achieve fast recording speed for *in vivo* imaging, the line scanning was performed in one dimension (*Y*-direction) for super-resolution imaging. A total of 255 line-profiles were acquired to reconstruct one super-resolution image. In this experiment, the imaging speed of the camera was set at 30,000 frames/s (fps), corresponding to a 100-fps speed for VSD-based super-resolution imaging.

A fiber-coupled light-emitting diode with a central wavelength at 505 nm (M505F1; Thorlabs, Inc.) was employed to produce the green flash used for retinal stimulation. The visible stimulation was obliquely delivered to the retina to elicit TRP [Fig. 1(b)] and its incident angle on the retina was adjusted by

*Address all correspondence to: Xincheng Yao, E-mail: xcy@uic.edu

1083-3668/2018/$25.00 © 2018 SPIE

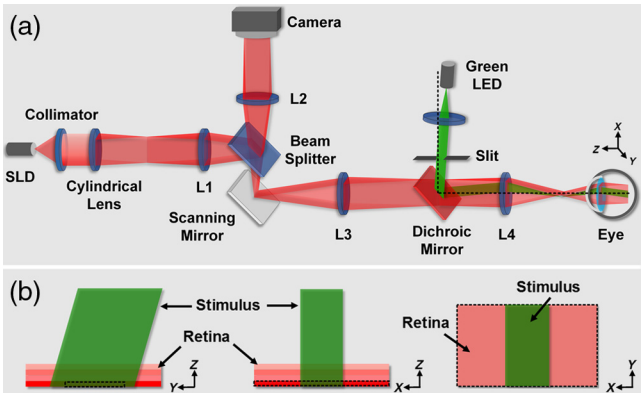

Fig. 1 (a) Schematic of the line-scan ophthalmoscope for *in vivo* super-resolution imaging. The illumination for retinal imaging is produced by a SLD. The line profile of illumination scanned across the retina is produced by the cylindrical lens. L1–L4 are lenses with focal lengths of 80, 400, 80, and 25 mm, respectively. The black dashed line represents the virtual optical axis for a perpendicular stimulation on the retina. The oblique stimulation is then achieved by applying an "off-axis" setup in the stimulation path. (b) Illustration of the oblique stimulation and retina: right-side view (left), front view (middle), and top view (right) of the oblique stimulation and retina. The black-dashed rectangles represent the imaging area on the photoreceptor layer of retina. (a) and (b) Share the same coordinates.

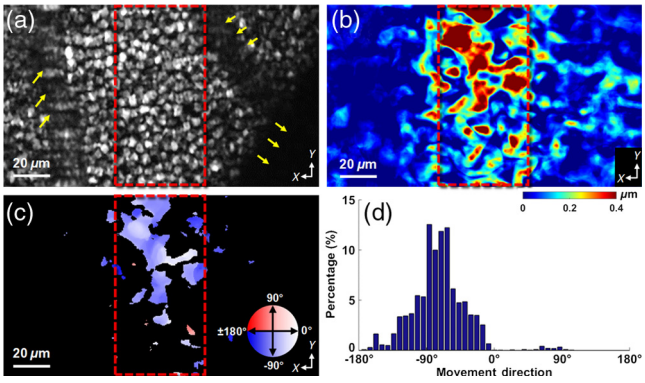

Fig. 2 *In vivo* TRP evoked by a localized oblique stimulation. (a) Representative *in vivo* super-resolution image of the photoreceptor layer (Video 1). Yellow arrowheads indicate retinal blood vessels. Representative magnitude map (b) and direction map (c) of photoreceptor movement recorded at time 0.4 s after the onset of stimulation. The inset color map in (c) shows the colors that represent different movement directions. The black area represents the retinal locations where no reliable movements can be detected. The red-dashed rectangles in (a), (b), and (c) represent the stimulated retinal area. (d) Histogram of movement directions in (c). (a), (b), and (c) Share the same coordinates with Fig. 1 (Video 1, MPEG, 287 KB [URL: https://doi.org/10.1117/1.JBO.23.5.050502.1]).

a kinetic mount (KC1; Thorlabs, Inc.) that held both the fiber tip and the collimator. To better distinguish the stimulus-evoked photoreceptor movement from background, only the retinal area at the center of the field of view was illuminated by the visible stimulation [middle and left panel in Fig. 1(b)]. The localized stimulation was achieved by placing a slit at the conjugate plane of the retina in the stimulation path [Fig. 1(a)]. The stimulating power was first measured by a power meter (PM200; Thorlabs, Inc.) placed at the rear focal plane of the lens before the eye [L4 in Fig. 1(a)] and was then converted to stimulation intensity on the retina.[16]

Figure 2 shows *in vivo* TRP correlated with oblique visible stimulation. Figure 2(a) shows a representative image of the photoreceptor layer acquired by the VSD-based super-resolution ophthalmoscope with an imaging speed of 100 frames/s and a field of view of 100 μm × 200 μm on the retina. Individual photoreceptors were clearly imaged with subcellular spatial resolution and millisecond temporal resolution, which allowed quantitative measurement and dynamic monitoring of photoreceptor movements. To elicit TRP, a rectangular stimulation pattern was obliquely projected onto the retina and stimulated a retinal area that has a width of ~50 μm at the center of the field of view [red-dashed rectangle in Fig. 2(a)].

To quantify TRP, we calculated the magnitude and direction map of photoreceptor movements based on the retinal images using the optical flow code developed by Sun et al.[17] Optical flow is a well-established method for measuring object movements between two images. Therefore, it can accurately identify the process of photoreceptor movement through sequential retinal images.[8,10] A 3-δ threshold and a temporal window generated from the movement magnitude maps were applied to exclude potential spatial and temporal noise in the movement direction map.[10,18] Figures 2(b) and 2(c) are representative magnitude and direction map of the photoreceptor movements evoked by the localized stimulation. As Figs. 2(b) and 2(c) match Fig. 2(a), the red-dashed rectangles shown in Figs. 2(b) and 2(c) also represent the stimulated retinal area. Therefore, Figs. 2(b) and 2(c) reveal that robust photoreceptor movements were primarily confined within the stimulated retinal region. The distribution of movement direction in Fig. 2(c) was further analyzed to illustrate the correlation between the directions of photoreceptor movements and oblique stimulation. As shown in Fig. 2(d), most stimulus-evoked photoreceptor movements had a direction close to −90 deg, indicating the photoreceptors moved toward the incident stimulation, which was consistent with our previous *in vitro* observation of TRP.[7,8,10]

To illustrate the spatiotemporal dynamics of TRP, representative magnitude and direction maps of photoreceptor movement selected from different phases of the experiment are shown in Fig. 3. As the stimulation onset was set as 0 s and the stimulation period lasted for 0.5 s, Fig. 3 covers the photoreceptor movements before, during, and after the stimulation. Figure 3(a) demonstrates that robust photoreceptor movements were only observed after the onset of stimulation and within the stimulated retinal area. Figures 3(b) and 3(c) further proved the direction of stimulus-evoked photoreceptor movement was consistently toward the direction of incident stimulation during and after the stimulation period. It was also noticed that some of the stimulated retinal regions did not present reliable movements during the recording period and some other regions presented opposite movement direction at certain time points [pink areas in Figs. 2(c) and 3(b)]. Similar phenomena were observed in our previous *in vitro* TRP studies using different imaging modalities, including OCT, confocal, and light microscopies.[8,10] These phenomena are speculated to be related to the complex structure of the retina, and accurate oblique stimulation and actual intensity control for each single photoreceptor are difficult due to inevitable light scattering and coherent mechanical interaction among neighboring photoreceptors.

The correlation between photoreceptor movement magnitude and stimulation intensity was further investigated. Three stimulation intensities, i.e., 1.97×10^5, 0.67×10^5, and 0.197×10^5 photons $\cdot$ $\mu m^{-2} \cdot ms^{-1}$, were tested as a pilot study. Our

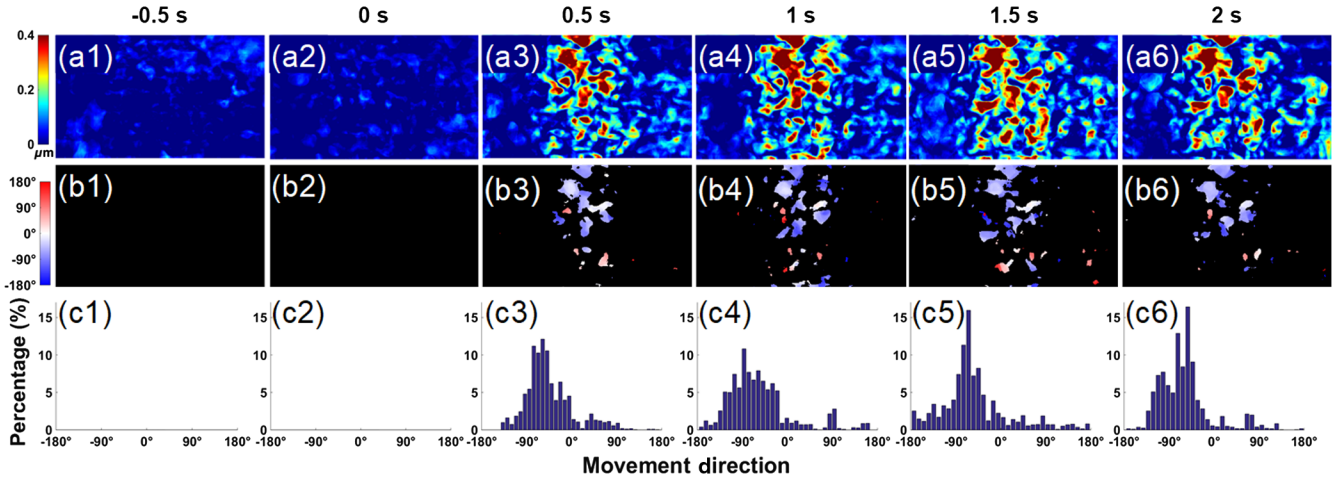

Fig. 3 Spatiotemporal dynamics of *in vivo* TRP evoked by localized oblique stimulation. Magnitude maps of photoreceptor movement obtained before (a1–a2), during (a3), and after (a4–a6) the stimulation (Video 2). Direction maps of photoreceptor movement obtained before (b1–b2), during (b3), and after (b4–b6) the stimulation (Video 3). (c) Histograms of the movement direction corresponded to the movement direction maps in (b). The stimulation started at time 0 s and lasted for 500 ms (Video 2, MPEG, 791 KB [URL: https://doi.org/10.1117/1.JBO.23.5.050502.2]; Video 3, MPEG, 336 KB [URL: https://doi.org/10.1117/1.JBO.23.5.050502.3]).

previous *in vivo* intrinsic optical signal (IOS) studies showed such stimulations could activate significant but different retinal responses.[19] The flash duration was set to 500 ms for eliciting robust photoreceptor movements. As the line-scan modality fulfilled a fast recording speed, a time-magnitude course was used to reflect the dynamics of photoreceptors with a 10-ms temporal resolution.[10] Figure 4 shows the results obtained from a group of six samples. Each trace in Fig. 4(a) is the mean of 12 time-magnitude courses and is accompanied by the standard deviations of data about the mean (colored area). The relationship of the standard deviation amplitudes to the waveform in each trace indicates general similarity between the results obtained from different samples. The waveforms of all three traces are flat and stable in the prestimulus phase and exhibit an immediate and significant rise upon the initiation of the stimulation. However, the waveforms also show that different stimulation intensity remarkably changed the response of the photoreceptor.

To better illustrate the difference caused by increasing stimulation intensity, two parameters, peak amplitude (the maximum value of photoreceptor movement magnitude) and time-to-peak (time taken to reach the peak amplitude) of the waveforms, were compared. The results in Fig. 4(b) show that the difference between peak amplitudes of the three traces was statistically insignificant, suggesting the peak amplitude is irrelevant to the variation of stimulation intensities within a certain range. However, as shown in Fig. 4(c), the time-to-peak values were significantly reduced by higher stimulus intensity, indicating brighter stimulus results in earlier saturation of the photoreceptor movement. These results suggested an intimate correlation between photoreceptor movement and phototransduction as the accelerated photoreceptor response might be the consequence of more rhodopsin and additional amounts of cascaded reactions activated by strong stimulation.[20] Similar effects were observed in our previous IOS and rod OS shrinkage studies, supporting that

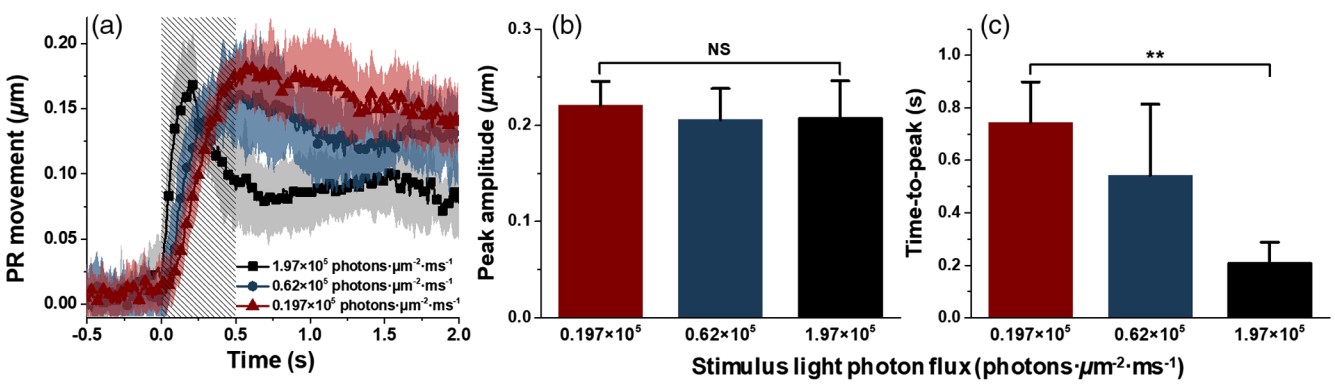

Fig. 4 Characteristics of photoreceptor movement correlated with stimulation intensities. (a) The time-magnitude courses of photoreceptor movement corresponded to three increasing stimulation intensities as, respectively, indicated by the legend. Each trace is an average of 12 datasets recorded from six different retinal samples. The colored area that accompanies each trace illustrates the standard deviations. Shaded area represents the 500-ms stimulation. PR: photoreceptor. The means and standard deviations of peak amplitude (b) and time-to-peak (c) of the traces in (a). Significance was determined by a one-way ANOVA with post-hoc Tukey honestly significant difference test for multiple comparisons, $^{**}p < 0.01$, NS, not significant, $n = 12$ retinal locations for each stimulus intensity.

photoreceptor movement is a major component of IOS and the unbalanced rod OS shrinkage is the mechanical source of TRP.[9,19,21]

In summary, this study demonstrated the feasibility of using a line-scan VSD-based super-resolution ophthalmoscope for *in vivo* imaging of TRP. Compared with traditional structure illumination microscopy, the VSD-based approach provides a compact, cost-efficient, and phase-artifact-free strategy to achieve super-resolution retinal imaging. The line-scan imaging modality achieved a fast recording speed for retinal activity. Corresponding to variable light intensity stimuli, it was observed that the TRP peak amplitude was not significantly sensitive to the stimulus light intensity, whereas TRP time-to-peak value was significantly sensitive to stimulus light intensity, i.e., reduced time-to-peak value corresponding to enhanced stimulus intensity. This observation indicates that the rod-dominated TRP was closely related to phototransduction in rod photoreceptors, and therefore reflected the functionality of rod photoreceptors. Further investigation of the *in vivo* properties of TRP may provide a high spatial resolution IOS imaging method for functional mapping of rod physiology. Our recent study has revealed a tight correlation between stimulus-evoked TRP and photoreceptor IOS changes in freshly isolated retinal tissues.[7] Previous studies have revealed IOS changes in both photoreceptors and inner retinal layers,[22–25] and emerging functional OCT enabled depth-resolved detection of photoreceptor IOS from inner retinal IOSs.[18,21] We anticipate that better investigation of the *in vivo* properties, including physical and physiological mechanisms and spatial and temporal dynamics, of stimulus-evoked TRP in animal models will provide valuable information for advanced instrument development and better stimulation protocol designs for pursuing *in vivo* IOS imaging of human retina, enabling early detection of AMD, in which rod photoreceptor dysfunction occurs first, and other eye diseases.

Disclosures

No conflicts of interest, financial or otherwise, are declared by the authors.

Acknowledgments

This research was supported in part by NIH R01 EY023522, NIH R01 EY024628, and NIH P30 EY001792.

References

1. G. R. Jackson, C. Owsley, and C. A. Curcio, "Photoreceptor degeneration and dysfunction in aging and age-related maculopathy," *Ageing Res. Rev.* **1**(3), 381–396 (2002).
2. D. Nagy et al., "Long-term follow-up of retinitis pigmentosa patients with multifocal electroretinography," *Invest. Ophthalmol. Visual Sci.* **49**(10), 4664–4671 (2008).
3. F. Billson et al., "Macular electroretinograms: their accuracy, specificity and implementation for clinical use," *Clin. Exp. Ophthalmol.* **12**(4), 359–372 (1984).
4. J. Li, M. O. Tso, and T. T. Lam, "Reduced amplitude and delayed latency in foveal response of multifocal electroretinogram in early age related macular degeneration," *Br. J. Ophthalmol.* **85**(3), 287–290 (2001).
5. C. Owsley et al., "Comparison of visual function in older eyes in the earliest stages of age-related macular degeneration to those in normal macular health," *Curr. Eye Res.* **41**(2), 266–272 (2016).
6. J. Siderov and A. L. Tiu, "Variability of measurements of visual acuity in a large eye clinic," *Acta Ophthalmol.* **77**(6), 673–676 (1999).
7. R. Lu et al., "Dynamic near-infrared imaging reveals transient phototropic change in retinal rod photoreceptors," *J. Biomed. Opt.* **18**(10), 106013 (2013).
8. B. Wang et al., "Functional optical coherence tomography reveals transient phototropic change of photoreceptor outer segments," *Opt. Lett.* **39**(24), 6923–6926 (2014).
9. X. Zhao et al., "Stimulus-evoked outer segment changes in rod photoreceptors," *J. Biomed. Opt.* **21**(6), 065006 (2016).
10. Y. Lu et al., "Stimulus-evoked outer segment changes occur before the hyperpolarization of retinal photoreceptors," *Biomed. Opt. Express* **23**(1), 38–47 (2017).
11. C. Liu et al., "In vivo super-resolution retinal imaging through virtually structured detection," *J. Biomed. Opt.* **21**(12), 120502 (2016).
12. Y. Lu, C. Liu, and X. Yao, "In vivo observation of transient photoreceptor movement correlated with oblique light stimulation," *Proc. SPIE* **10497**, 104971M (2018).
13. F. C. Delori, R. H. Webb, and D. H. Sliney, "Maximum permissible exposures for ocular safety (ANSI 2000), with emphasis on ophthalmic devices," *J. Opt. Soc. Am. A* **24**(5), 1250–1265 (2007).
14. I. E. Commission, *IEC 60825-1 Safety of Laser Products-Part 1: Equipment Classification and, Requirements*, International Electrotechnical Commission, Geneva, Switzerland (2001).
15. D. J. Fechtig et al., "Line-field parallel swept source MHz OCT for structural and functional retinal imaging," *Biomed. Opt. Express* **6**(3), 716–735 (2015).
16. R. Douglas and N. Marshall, "A review of vertebrate and invertebrate ocular filters," in *Adaptive Mechanisms in the Ecology of Vision*, pp. 95–162, Springer, Dordrecht (1999).
17. D. Sun, S. Roth, and M. J. Black, "Secrets of optical flow estimation and their principles," *Comput. Vision Pattern Recognit*, 2432–2439 (2010).
18. Q. Zhang et al., "Functional optical coherence tomography enables in vivo physiological assessment of retinal rod and cone photoreceptors," *Sci. Rep.* **5**, 9595 (2015).
19. Q. X. Zhang et al., "In vivo confocal intrinsic optical signal identification of localized retinal dysfunction," *Invest. Ophthalmol. Vis. Sci.* **53**(13), 8139–8145 (2012).
20. V. Y. Arshavsky, T. D. Lamb, and E. N. Pugh Jr., "G proteins and phototransduction," *Annu. Rev. Physiol.* **64**(1), 153–187 (2002).
21. B. Wang, Y. Lu, and X. Yao, "In vivo optical coherence tomography of stimulus-evoked intrinsic optical signals in mouse retinas," *J. Biomed. Opt.* **21**(9), 096010 (2016).
22. Y.-C. Li et al., "Parallel optical monitoring of visual signal propagation from the photoreceptors to the inner retina layers," *Opt. Lett.* **35**(11), 1810–1812 (2010).
23. X. Yao and B. Wang, "Intrinsic optical signal imaging of retinal physiology: a review," *J. Biomed. Opt.* **20**(9), 090901 (2015).
24. X.-C. Yao, "Intrinsic optical signal imaging of retinal activation," *Jpn. J. Ophthalmol.* **53**(4), 327–333 (2009).
25. X. C. Yao and Y. B. Zhao, "Optical dissection of stimulus-evoked retinal activation," *Opt. Express* **16**(17), 12446–12459 (2008).